

Dynamic phenotypic switching and group behavior help non-small cell lung cancer cells evade chemotherapy

Arin Nam¹, Atish Mohanty¹, Supriyo Bhattacharya², Sourabh Kotnala¹, Srisairam Achuthan², Kishore Hari³, Saumya Srivastava¹, Linlin Guo¹, Anusha Nathan¹, Rishov Chatterjee², Maneesh Jain⁴, Wasim Nasser⁴, Surinder Batra⁴, Govindan Rangarajan³, Erminia Massarelli¹, Herbert Levine⁵, Mohit Kumar Jolly³, Prakash Kulkarni¹, and Ravi Salgia¹

¹City of Hope National Medical Center Department of Medical Oncology and Therapeutics Research

²City of Hope Comprehensive Cancer Center Duarte

³Indian Institute of Science

⁴University of Nebraska Medical Center

⁵Northeastern University College of Engineering

March 07, 2024

Abstract

Drug resistance, a major challenge in cancer therapy, is typically attributed to mutations and genetic heterogeneity. On the other hand, emerging evidence suggests that dynamic cellular interactions and group behavior also contribute to drug resistance. However, the underlying mechanisms remain poorly understood. Here, we present a new mathematical approach with game theoretical underpinnings that we developed to model real-time growth data of non-small cell lung cancer (NSCLC) cells and discern patterns in response to treatment 68 with cisplatin. We show that the cisplatin-sensitive and cisplatin-tolerant NSCLC cells when co69 cultured in the absence or presence of the drug, display dynamic group behavior strategies. Tolerant cells exhibit a ‘persister-like’ behavior and are attenuated by sensitive cells; they also appear to ‘educate’ sensitive cells to evade chemotherapy. Further, tolerant cells can switch phenotypes to become sensitive, especially at low cisplatin concentrations. Finally, switching treatment from continuous to an intermittent regimen can attenuate the emergence of tolerant cells, suggesting that intermittent chemotherapy may improve outcomes in lung cancer.

1
2 **Dynamic phenotypic switching and group behavior help non-small cell lung**
3 **cancer cells evade chemotherapy**
4

5 Arin Nam^{1†}, Atish Mohanty^{1†}, Supriyo Bhattacharya^{2†}, Sourabh Kotnala¹, Srisairam Achuthan³
6 Kishore Hari⁴, Saumya Srivastava¹, Linlin Guo¹, Anusha Nathan^{1¶}, Rishov Chatterjee³, Maneesh
7 Jain⁵, Mohd W Nasser⁵, Surinder K Batra⁵, Govindan Rangarajan^{6,7}, Erminia Massarelli¹, Herbert
8 Levine^{8,9}, Mohit Kumar Jolly⁴, Prakash Kulkarni¹, Ravi Salgia^{1*}
9

10 ¹Department of Medical Oncology and Therapeutics Research, City of Hope National Medical
11 Center, Duarte, CA 91010, USA, ²Translational Bioinformatics, Center for Informatics,
12 Department of Computational and Quantitative Medicine, City of Hope National Medical
13 Center, Duarte, CA 91010, USA, ³Center for Informatics, Division of Research Informatics, City of
14 Hope National Medical Center, Duarte, CA 91010, USA, ⁴Center for BioSystems Science and
15 Engineering, Indian Institute of Science, Bangalore 560012, India, ⁵Department of Biochemistry
16 and Molecular Biology, College of Medicine, University of Nebraska Medical Center, Omaha, NE,
17 USA, ⁶Department of Mathematics, and ⁷Center for Neuroscience, Indian Institute of Science,
18 Bangalore 560012, India, ⁸Department of Physics and ⁹Department of Bioengineering,
19 Northeastern University, Boston, MA 02115, USA
20
21
22

23 ***Corresponding Author:** Dr. Ravi Salgia, MD, PhD
24 Professor and Chair
25 Department of Medical Oncology and Therapeutics Research
26 Arthur & Rosalie Kaplan Endowed Chair in Medical Oncology
27 Associate Director of Clinical Services
28 1500 E. Duarte Road, Duarte, CA 91010-3000
29 Phone 626-471-9200, Fax 626-471-7322
30 Email: rsalgia@coh.org
31

32 [†]These three authors contributed equally to this work and hence, they should be considered as
33 co-first authors.

34 [¶]**Present address:** Harvard Medical School, 25 Shattuck St, Boston, MA 02115, USA

35 **Declaration of Interest and Financial Disclosures:** The authors declare they have no conflict of
36 interests or any financial disclosures

37 **Animal Welfare Assurances:** All zebrafish studies were approved by City of Hope (COH)
38 Institutional Animal Care and Use Committee (IACUC), and all experiments were performed

39 conforming to the relevant regulatory standards under protocol IACUC# 18119. The zebrafish
40 larvae used for microinjections were 48 h old i.e., 2 days post fertilization (dpf), and were
41 continuously observed for tumor development until 7 dpf. During this period, no sex
42 differentiation is observed. Ovarian development is the default pathway, which is initiated at 10
43 dpf and around 21 dpf sexual differentiation into females and males is established. The two cell
44 lines used for microinjections were H2009 and H23. The cell lines were obtained from ATCC.
45 H2009 is an adenocarcinoma cell line derived from a 68-year-old female patient and H23 is
46 another adenocarcinoma cell line derived from a 51-year-old male patient.

47

48 **Code Availability:** The codes used in our data analysis have been deposited in a private
49 repository on Github. This will be made public once the article is accepted. However, to share it
50 with the reviewers, we have prepared a Google Drive folder containing the compressed files of
51 the private GitHub repository
52 (<https://drive.google.com/drive/folders/1AcT6gd8pOokq6uTCQlGiGscUNYOnMoBq?usp=sharing>
53 g). Once unzipped, the README.md file within the master directory will give all code viewers
54 clear directions and guidance for navigating sub-directories and running all relevant codes for
55 models used in the manuscript.”

56

57 **Running title:** Modeling chemoresistance

58

59 **Key Words:** chemoresistance, cisplatin, lung cancer, evolutionary game theory, group behavior,
60 persister trait, phenotypic switching

61 **Summary**

62 Drug resistance, a major challenge in cancer therapy, is typically attributed to mutations
63 and genetic heterogeneity. On the other hand, emerging evidence suggests that dynamic
64 cellular interactions and group behavior also contribute to drug resistance. However, the
65 underlying mechanisms remain poorly understood. Here, we present a new mathematical
66 approach with game theoretical underpinnings that we developed to model real-time growth
67 data of non-small cell lung cancer (NSCLC) cells and discern patterns in response to treatment
68 with cisplatin. We show that the cisplatin-sensitive and cisplatin-tolerant NSCLC cells when co-
69 cultured in the absence or presence of the drug, display dynamic group behavior strategies.
70 Tolerant cells exhibit a ‘persister-like’ behavior and are attenuated by sensitive cells; they also
71 appear to ‘educate’ sensitive cells to evade chemotherapy. Further, tolerant cells can switch
72 phenotypes to become sensitive, especially at low cisplatin concentrations. Finally, switching
73 treatment from continuous to an intermittent regimen can attenuate the emergence of
74 tolerant cells, suggesting that intermittent chemotherapy may improve outcomes in lung
75 cancer.

76

77 Introduction

78 Drug resistance in cancer is generally believed to arise stochastically through random
79 genetic mutations and the subsequent expansion of mutant clones via Darwinian selection.^{1,2}
80 However, emerging evidence suggests that non-genetic and epigenetic mechanisms may also
81 play a critical role³⁻⁵, leading to enhanced adaptability and cooperation under stressful
82 conditions.³⁻⁵ Nonetheless, such mechanisms have not been fully explored and are rarely
83 integrated into clinical trials or in precision oncology initiatives.⁶⁻⁸ Furthermore, combining
84 conventional therapies with treatment strategies based on cancer ecology could potentially
85 delay or even prevent drug tolerance and eventually, drug resistance.^{2,8-10}

86 Several studies have reported the existence of drug-resistant and tolerant (clones that
87 are weakly or moderately resistant) clones in pre-treatment tumors¹¹, although the population
88 of these clones is usually low in the presence of drug-sensitive cells¹². This raises the question,
89 how do drug-sensitive and resistant/tolerant clones in a tumor influence each other's fitness
90 (growth), and whether cooperation and competition (group behavior) between the sensitive
91 and tolerant cells influence the response to drug therapy. Thus, discerning group behavior by
92 monitoring interactions between drug-tolerant and -sensitive cells in real time in absence or
93 presence of the drug is a powerful tool to elucidate the role of group behavior.^{13,14}

94 Here, we have used human non-small cell lung cancer (NSCLC) cells that are sensitive or
95 tolerant to cisplatin, one of the most commonly used chemotherapy, to understand the role of
96 group behavior in emergence of drug-tolerant clones, and eventually resistant clones. The cells
97 expressing red fluorescent protein (RFP) or green fluorescent protein (GFP) were mixed
98 (heterotypic culture) and cultured in different ratios. The proliferation of the two cell types was
99 followed in real time and compared to the same cells grown alone (monotypic culture). The cell
100 counts were used to determine the dynamic behavior of the population, and results were
101 correlated with the cell-autonomous and non-cell-autonomous fitness (growth rate) effects⁵.
102 Since cell-autonomous fitness effects are defined as those inherent to the cell, the growth rates
103 from monotypic cultures provided the necessary information for determining these effects.⁴ In
104 contrast, non-cell-autonomous effects are those that allow fitness to depend on a cell's
105 microenvironment including the frequency of other cellular phenotypes as well as diffusible
106 factors in the media.¹⁵

107 Since standard models based on evolutionary game theory proved inadequate to
108 analyze the data, we developed a new approach, Phenotypic Switch Model with Stress
109 Response (PSMSR), that incorporates concepts from chemical reaction kinetics and the
110 cooperative behavior of drug-tolerant phenotypes in the community. A distinguishing feature of
111 the PSMSR model is that it considers the ability of cancer cells to switch phenotypes. Employing
112 PSMSR, we showed that quantitatively, the two cell populations when co-cultured in the
113 absence of cisplatin, display dynamic group behavior that can be interpreted using evolutionary
114 game theory as payoffs (benefit or loss of individual players associated with a set of game
115 strategies such as competition or cooperation). Due to phenotypic switching by the cells, the
116 game strategies were dynamically altered based on cell frequencies and stress level while
117 maximizing group survival. However, in presence of cisplatin, the group behavior (cooperation)

118 was attenuated in favor of self-survival. Furthermore, we demonstrate that switching
119 treatments from a continuous to an intermittent regimen can attenuate the emergence of
120 tolerant cells, underscoring a potentially new treatment option that could benefit patients with
121 NSCLC.

122 **Results**

123 *Cisplatin-sensitive and tolerant cells demonstrate different behaviors in monotypic and* 124 *heterotypic cultures*

125 A schematic overview summarizing the experiments and the source of data collection
126 used in developing the theoretical models are presented in **Fig.1A-C**. Fluorescently labeled
127 cisplatin-sensitive H23 and cisplatin-tolerant H2009 NSCLC cells¹⁶ were co-cultured and
128 monitored in real time (**Supplementary Fig. 1A & B**). To discern differences in their behavior,
129 the two cell cultures were grown as monotypic or as heterotypic cultures in a 1:1 ratio. To
130 determine the short-term effects of heterotypic culture, we incubated the cells for 12 h before
131 the start of the experiment (**Supplementary Fig. 2A**, schematic). But to determine the long-
132 term effects, they were co-cultured for 3 weeks (without cisplatin) before the start of the
133 experiment (**Fig. 2A**, schematic).

134 At a 1:1 ratio, there was no significant difference in the fold-change (ratio of the cell
135 population at any time point relative to $t = 0$ hours) of the sensitive cell counts between the
136 monotypic (grown by themselves) and heterotypic cultures (mixed with tolerant cells for 12 h
137 or 3 weeks prior to counting), and they were equally sensitive to 5 μ M cisplatin in all three
138 conditions (**Fig. 2A**, left panel bar graph in red). These monotypic and heterotypic culture
139 experiments were also performed using tolerant cells, and no significant change in cell count or
140 drug tolerance was observed for the cells mixed only for 12 h prior to the experiment (**Fig. 2A**,
141 right panel bar graph in green, bars labeled “Alone” and “Mix before”). However, when tolerant
142 cells were co-cultured with sensitive cells for 3 weeks prior to the experiment, they showed a
143 marked reduction in cell proliferation (**Fig. 2A** green bar graph, dark green bar labeled “3-wk co-
144 culture”). Moreover, when cisplatin was added to this 3-week co-cultured cells, the tolerant
145 cells showed a smaller reduction in cell growth compared to when cultured separately or mixed
146 12 h before the experiment was started (**Fig. 2A**, right panel bar graph in green), and their
147 proliferation was significantly attenuated by long coexistence with the sensitive cells,
148 suggesting that tolerant cells appear to exhibit a ‘persister-like’ trait (please see the
149 “Discussion” section).^{17,18}

150 We further explored the long term 3-week co-culture experiments by seeding the cells
151 at increasing tolerant to sensitive ratios (1:1, 2:1, 4:1, 8:1), and recorded their growth every 2 h
152 using the IncuCyte live cell imaging system (**Supplementary Fig. 1C** schematic). At a seeding
153 ratio of 1:1, the sensitive cells showed an 8-fold increase in cell count within 96 h, and reached
154 a plateau post 96 h, whereas the tolerant cells exhibited a 4-fold increase in cell count within 72
155 hours, followed by a drop and plateau for the rest of the time (**Fig. 2B**). At the end of the
156 experiment i.e. 144 h, the sensitive cell growth was 2.5-fold more than the tolerant cells for 1:1
157 ratio, compared to 1.5, 1.4 and 1.2-fold for the 2:1, 4:1 and 8:1 ratios, respectively (**Fig. 2C**).

158 These data revealed that the tolerant cell proliferation was suppressed in presence of sensitive
159 cells but could be rescued by increasing the fraction of tolerant cells in the co-cultures.

160 Next, we determined the proliferation profile for all the seeding ratios in presence of
161 cisplatin. Cisplatin had a cytostatic effect on the sensitive cells, and the fold change in the cell
162 count remained approximately 1 for all the ratios (**Fig. 2D**, purple bar graph). However, the
163 tolerant cell proliferation was approximately 1.4, 2.09, 1.95, and 2.04 fold at the
164 tolerant:sensitive seeding ratios 1:1, 2:1, 4:1 and 8:1, respectively. Therefore, the
165 administration of cisplatin rescued the tolerant cell growth from the suppressive effect of the
166 sensitive cells by selectively curtailing the sensitive cell growth. In fact, the tolerant cells
167 proliferated better in the presence of cisplatin and increasing the seeding ratio of tolerant cells
168 in the population also favored their growth (**Fig. 2D**).

169 The suppressive effect of the sensitive cells on the tolerant cells in a frequency-
170 dependent manner was also evident by analyzing the change in tolerant to sensitive fraction at
171 the end of 144 hours in the untreated conditions (0.2, 1.4, 6.3, 17.4 at T:S seeding ratios of 1:1,
172 2:1, 4:1 and 8:1, respectively, **Fig. 2E**, black bars). In addition, the tolerant to sensitive fractions
173 in presence of cisplatin were 0.8, 4.9, 16.9 and 38.8 for the same seeding ratios (**Fig. 2E**, orange
174 bars). Thus, there was an increase in the tolerant to sensitive cell fraction in the population
175 treated with cisplatin, suggesting a reduction in the sensitive cell population as well as better
176 fitness of the tolerant cells in presence of cisplatin.

177 *Sensitive cells suppress growth of tolerant cells in absence of drug*

178 To discern the effect of short-term association between the sensitive and the tolerant
179 cells on their group behavior, we repeated the above experiments by incubating the co-culture
180 for only 12 h instead of 3 weeks prior to starting the experiments (**Supplementary Fig. 2A**,
181 schematic). Here, at 1:1 tolerant:sensitive seeding ratio, the fold change in the tolerant cell
182 population at the end of 144 h was 8-fold (**Supplementary Fig. 2B**), whereas after three weeks
183 of co-culture, we observed a 4 fold change in the growth (**Fig. 2C and Supplementary Table 1**).
184 Also, compared to the 3 weeks co-culture, where the tolerant cell fold changes were
185 significantly lower ($p < 0.0001$) than that of the sensitive cells for all seeding ratios except 8:1,
186 the 12-hour co-culture showed less difference in fold changes between the two cell types ($p <$
187 0.001) at seeding ratios 2:1 and 4:1, and insignificant at 8:1 (**Supplementary Fig. 2E**). The
188 tolerant to sensitive fraction in the population at 144 hours was also higher than in the 3 weeks
189 co-culture experiments for seeding ratios 1:1 and 2:1 (1.2 and 3.3 vs. 0.2 and 1.4 in the 3 weeks
190 co-culture, **Supplementary Fig. 2G**). Taken together, these data show that the short-term
191 association between the two cell types did not suppress the tolerant cell population as
192 efficiently as the long-term association. However, in presence of cisplatin, the tolerant cell
193 proliferation was significantly higher compared to the sensitive cells ($p < 0.0001$, **Supplementary**
194 **Fig. 2C and F**). Next, we compared the change in the tolerant cells to the sensitive cell fraction
195 and observed a similar trend as seen in the 3 weeks co-culture for all seeding ratios. The
196 increase in growth of the tolerant cells was also supported by the increase in their fraction in
197 the population in absence of cisplatin, and further the presence of cisplatin supported their
198 growth. (**Supplementary Fig. 2C, 2D orange line graph and 2G orange bar graph**).

199 The growth trends indicated a competition between the two cell types which was
200 enhanced by long-term association. In contrast, the behavior of the tolerant cells suggested
201 mutual cooperation to improve survival, which was favored by the higher seeding ratios. To
202 explore the frequency-dependent competition of the sensitive cells towards the tolerant cells,
203 we expanded the seeding ratios to increased proportions of sensitive cells in the population
204 (i.e. sensitive to tolerant ratios of 1:1 to 8:1) (**Supplementary Fig. 3A**, schematic).

205 Consistent with the previous experiments, in the absence of cisplatin, the sensitive cells
206 suppressed the growth of tolerant cells (**Supplementary Fig. 3B** and **E**). Again, in the presence
207 of cisplatin, the tolerant cell growth was dominated in the population by approximately 1.9, 2.2,
208 2.7 or 3.8-fold over sensitive cells for the sensitive to tolerant ratios of 1:1, 2:1, 4:1 or 8:1,
209 respectively (**Supplementary Fig. 3F**). The increase in growth of the tolerant cells was also
210 supported by the presence of cisplatin (**Supplementary Fig. 3C,3D orange line graph and 3G**
211 **orange bar graph**). Together, these experiments indicated that in a heterogeneous population,
212 dynamic competition and cooperation exist between the sensitive and the tolerant cells, and
213 the sensitive cells dominate over the tolerant cells. In contrast, the presence of cisplatin favors
214 the survival and proliferation of the tolerant cells by inducing cell death among the sensitive
215 cells.

216 *Sensitive cells secrete a factor(s) that retards the growth of tolerant cells*

217 To discern whether a physical interaction between the two cell types is necessary for
218 this, or the sensitive cells secrete an 'inhibitory factor' to attenuate tolerant cell growth, the
219 cells were grown in conditioned medium from sensitive or tolerant cell monocultures (**Fig. 2F**,
220 schematic). As seen in the right graph in **Fig. 2G**, conditioned medium from the sensitive cells
221 impeded proliferation of tolerant cells by ~4.5-fold. In contrast, the conditioned medium from
222 the tolerant cells had no significant effect on the growth of the sensitive cells (**Fig. 2G**, left
223 graph), alluding to the presence of one or more inhibitory factors in the conditioned medium
224 from the sensitive cells. Furthermore, at a lower seeding density (**Fig. 2H**, schematic), the
225 conditioned medium had a greater inhibitory effect (approximately 6-fold) on the tolerant cells
226 and reduced in a dose-dependent fashion with an increase in tolerant cell seeding density (**Fig.**
227 **2I**). Thus, the suppressive effect of the sensitive cell-conditioned medium was reduced with a
228 greater number of tolerant cells (**Fig. 2I**).

229 *Intermittent therapy can sustain a population of cisplatin-sensitive tumor cells while attenuating*
230 *the proliferation of resistant cells*

231 Since the proliferation of the tolerant cells was remarkably impeded when co-cultured
232 with sensitive cells for prolonged periods prior to cisplatin treatment, we asked if continuous or
233 intermittent cisplatin treatments would differentially affect a mixed population of the two cell
234 types. Toward this end, we mixed the two cell types at different sensitive to tolerant ratios and
235 treated them as described in **Supplementary Fig. 4**, schematic. Within 10 days, we observed
236 that the ratio of tolerant to sensitive cells increased by 50- to 100-fold for the initial seeding
237 ratios of 1:1, 2:1 and 4:1 (sensitive:tolerant), respectively, under continuous treatment. On the
238 other hand, the tolerant to sensitive (T:S) ratio for the intermittent therapy increased only 3- to

239 8-fold (**Fig. 3A-C**), suggesting that sensitive cells were able to recover from the drug toxicity and
240 proliferate.

241 We prolonged the intermittent therapy by splitting the cells growing in cisplatin-free
242 media post cisplatin treatment into two sets: 'Intermittent 1 cycle' and 'Intermittent 2 cycles' as
243 described **Supplementary Fig. 4**. In 'Intermittent 1', we observed the (initially cisplatin exposed)
244 cells cisplatin free for 25 days, whereas in 'Intermittent 2', we treated the cells with one extra
245 dose of cisplatin for 4 days, before observing them in cisplatin-free media for the rest of the
246 duration. We then asked if the sensitive cells once exposed to cisplatin would outgrow the
247 tolerant cells to recapitulate the data shown in **Fig. 2B** and **Supplementary Fig. 3B**.

248 We continued the culture for 24 days, to let the cells grow and once confluent, passaged
249 1 to 5 every 6-8 days. We observed that the tolerant vs. sensitive ratio fell to approximately 2,
250 1.6 and 0.4 for initial seeding densities of 1:1, 2:1 or 4:1, respectively, for the cells treated only
251 once with cisplatin on Day 3 (Intermittent – 1 cycle) (**Fig. 3D-F**, black line). In contrast, the ratio
252 of cells that received the 2nd dose of cisplatin treatment ('Intermittent – 2 cycles') and were
253 allowed to recover in fresh media, did not show any decrease in the tolerant population and
254 maintained a S:T ratio of 100/800 (**Fig. 3D-F**, red line). To validate the *in vitro* observations *in*
255 *vivo*, we injected zebrafish larvae with fluorescently tagged cells and treated them with
256 cisplatin (see **Supplemental Information** for details). While continuous cisplatin treatment for 5
257 days resulted in a tumor with predominantly tolerant cells, intermittent treatment led to no
258 significant change in the T:S ratio (**Fig. 3G**), indicating that intermittent treatment can ensure a
259 stable disease whereas the continues therapy favors emergence of drug refractory disease.

260 *Epigenetic modulation can distinguish drug sensitivity, tolerance and resistance in lung cancer*
261

262 To test the possibility that drug sensitivity can be regulated at the epigenetic level in a
263 reversible way, as opposed to genetic mutations alone, we used two different epigenetic
264 modulators namely, 5-azacytidine (5-AZA), a DNA methyltransferase inhibitor, and
265 suberoylanilide hydroxamic acid (SAHA), a histone deacetylase inhibitor, and determined their
266 effects on cisplatin resistance. While SAHA treatment did not enhance the effect of cisplatin on
267 sensitive H23 cells (**Fig. 3H**) or H1993 cells that are resistant to cisplatin ($IC_{50} > 300 \mu M$) (**Fig. 3J**),
268 it had a significant additive effect on the H2009 cells, suggesting that these cells can become
269 sensitive through epigenetic intervention (**Fig. 3I**). However, 5-AZA had no discernable effect
270 (not shown), suggesting that epigenetic regulation of chromatin rather than specific cytosine
271 residues in the DNA modulates cisplatin tolerance in the H2009 cells. Based on these criteria,
272 H2009 qualify as cisplatin-tolerant (reversible) rather than resistant (irreversible) while H1993
273 may represent a truly resistant phenotype. Taken together, these observations suggest that
274 tolerance to cisplatin can be reversed unless the tolerant cells acquire mutations making them
275 irreversibly resistant.

276

277 *Modeling cancer group behavior using experimentally derived growth curves*

278 Typically, group behavior among cancer cell populations is studied using variants of the
279 Lotka-Volterra (LV) model, where the inter-species competition and cooperation depend on the
280 species frequencies¹⁹⁻²¹. We tested one such model (Li et al) which has been successful in
281 explaining the evolutionary dynamics in bacterial co-cultures²². The major difference of the Li
282 et al model to LV is the implementation of growth rates that depend on the species
283 frequencies, leading to more complex dynamics than what could be captured by the classical LV
284 model. However, the Li et al model did not quantitatively explain our experimental data (details
285 in the **Supplementary text, Section 1 and Supplementary Fig. 5**) warranting alternative and
286 possibly more complex models. We think the models like LV or Li et al are not suitable for our
287 system partly due to the fact that they treat each cell identity as immutable, therefore ignoring
288 the plastic phenotypes of cancer cells due to phenotypic switching. To address these
289 deficiencies, we have developed a new model (Phenotype Switch Model with Stress Response
290 or PSMSR), incorporating the knowledge about our specific cellular system and the observed
291 growth trends.

292

293 The key evidence that motivated the new model PSMSR are as follows:

294 *(1) Sensitive cells suppress the proliferation of the tolerant cells by secreting diffusible*
295 *factors (can be overcome by increasing the frequency of tolerant cells)*

296

297 *(2) The suppressive effect is only prominent after co-culture of the two cell types for*
298 *three weeks, not if the cells are mixed and monitored immediately*

299

300 *(3) Competition by the sensitive cells is eliminated in presence of cisplatin, and*

301

302 *(4) Epigenetic modifier SAHA can switch the tolerant cells to be drug-sensitive through*
303 *non-genetic means, implying that these cells can switch their phenotypes in response to the*
304 *environment.*

305

306 Based on the above observations, the following are the key premises involved in PSMSR (**Fig.**
307 **4A**):

308

309 (1) Sensitive cells generate one or more products that affect the proliferation of the
310 tolerant cells (and possibly their own as well). We call this hypothetical product(s) 'stress' (we
311 explain its significance in **Supplementary Text Section 2**).

312

313 (2) Since the cohabitation of the cells appear to change their phenotypes (e.g. stronger
314 suppression of tolerant cells by the sensitive cells after three weeks of co-culture), and we do
315 not have enough information to model this phenotypic change as function of the cohabitation
316 conditions, every system (i.e. monotypic, heterotypic-12 h and heterotypic-3 weeks) must be
317 treated as distinct with their own phenotypic parameters.

318

319 (3) Through mutual cooperation, the tolerant cells can mitigate or neutralize the ‘stress’
320 generated by the sensitive cells in a frequency-dependent manner.

321
322 (4) Due to the stochastic phenotypic switching (sensitive \rightleftharpoons tolerant) by the two cellular
323 species, a state of equilibrium exists between the two phenotypes at any point of time, where
324 the equilibrium constant depends on the stress. As stress increases in the system, the
325 equilibrium shifts to the right to increase the fraction of the tolerant phenotype.

326 The model presented here reflects the following mechanisms: i) cellular growth leads to
327 stress accumulation, ii) accumulated stress reduces growth, iii) tolerant cells are efficient in
328 neutralizing stress, iv) stress accumulation triggers the switching of sensitive cells to the
329 tolerant phenotype. Hence, the growth rates of the sensitive (S) and the tolerant cells (T) can be
330 expressed as,

$$\frac{dS}{dt} = -K_a S + K_b T + K_{GS} S \quad (1)$$

331

$$\frac{dT}{dt} = -K_b T + K_a S + K_{GT} T \quad (2)$$

332 Here, K_{GS} and K_{GT} are the stress-dependent effective growth rates (incorporating both
333 proliferation and cell death) of the sensitive and tolerant cells respectively. K_a and K_b are the
334 rate of switching from sensitive to the tolerant phenotype and vice versa and K is the
335 equilibrium constant of phenotypic switching (eqn. 3).²³ We assume K_{GS} , K_{GT} , K to be linearly
336 dependent on stress and K_b to be fixed, although the exact functional forms that map these
337 quantities to stress is less important, as long as a monotonic relationship is maintained.
338 Notably, we also fit the PSMSR model assuming sigmoidal as opposed to linear relationships of
339 the above rate parameters with stress (**Supplementary Fig. 6**), without significant worsening of
340 fitting error (**Supplementary Fig. 7**). For details, see **Supplementary section 3**.

341 $K = \frac{K_a}{K_b}$ (3), where K is the equilibrium constant for phenotypic switching.

342 Next, we assume that stress is predominantly generated by the fast-growing sensitive
343 cells at a rate proportional to the cell population and neutralized by the tolerant cells. The
344 resulting rate equation is given by:

$$\frac{dC_{Str}}{dt} = K_{Str} S - K_{Str,d} T \quad (4)$$

345 where C_{Str} is a hidden variable representing the stress level, and K_{Str} and $K_{Str,d}$ are the rates of
346 stress generation and removal, respectively.

347 *PSMSR and cisplatin response*

348 To model the effect of cisplatin, we added a cisplatin dose-dependent cellular death
349 rate term to equations 1 and 2 to obtain equations 5 and 6. AUC stands for “area under the
350 curve” (AUC = cisplatin concentration x time of exposure), which represents the memory effect
351 of cisplatin exposure on the cellular growth (**Fig. 5A** and **Supplementary Text Section 2**).²⁴⁻²⁶
352 *Sigmoid(AUC)* is the sigmoidal function (equation 7) that varies between 0 and 1, depending on
353 the magnitude of AUC, which multiplied by the scale factor SCALE gives the cellular death rate.

354 AUC₅ and AUC₉₅ represent the AUC values where 5% and 95% of the cisplatin death effect are
 355 achieved respectively. The SCALE, AUC₅ and AUC₉₅ parameters are specific for the sensitive and
 356 the tolerant cell types.

$$357 \frac{dS}{dt} = -K_a S + K_b T + K_{G_s} S - SCALE_s \times \text{sigmoid}(AUC) \times S \quad (5)$$

$$358 \frac{dT}{dt} = -K_b T + K_a S + K_{G_t} T - SCALE_t \times \text{sigmoid}(AUC) \times T \quad (6)$$

$$359 \text{sigmoid}(AUC) = \left\{ 1 + \exp \left[\ln 19 \left(1 - 2 \frac{AUC - AUC_5}{AUC_{95} - AUC_5} \right) \right] \right\}^{-1} \quad (7)$$

360 In total, the PSMSR includes 9 unknown parameters (16, when including cisplatin effect). We
 361 used roughly 2900 cell population data collected over several days of cellular growth under
 362 various conditions to fit (**Fig. 4B-C**) and analyze the model parameters. The fitting was
 363 performed using the global optimization method, Genetic Algorithm (GA)²⁷, as implemented in
 364 the package GA in R.²⁸ (also see **Supplementary text Section 2**). The suitability of the PSMSR
 365 model in describing the experimental observations was assessed by constructing the log
 366 likelihood profiles for each parameter as described in **Supplementary text Section 4 and**
 367 **Supplementary Figs. 8-9**.

368 *PSMSR in monotypic and heterotypic cultures*

369 Our experimental observations indicated that the sensitive and the tolerant cells behave
 370 quite differently when cultured alone, as opposed to being in presence of one another
 371 (**Supplementary Fig. 10A-C**). Therefore, by deconvoluting the growth trends using PSMSR, we
 372 examined whether a few or all parameters of the model are different between the monotypic
 373 and the heterotypic cultures. In general, several phenotypic parameters for the heterotypic
 374 cultures were different in magnitude compared to the values for the monotypic cultures
 375 (**Supplementary Fig. 10J**). This indicates an influence of the cellular phenotypes on each other.
 376 The parameters that showed a consistent difference between the mono- and heterotypic
 377 cultures include K₀ and K_b (the parameters for phenotypic switching), K_{Gt0} (growth rate for the
 378 tolerant phenotype) and K_s (rate of stress generation). One interesting observation is that the
 379 growth rate for the tolerant phenotype in monotypic and 3-week co-cultures is 7-10 times
 380 smaller than that of the sensitive phenotype (**Supplementary Fig. 10J**), reminiscent of the
 381 persister trait (please see “Discussion”).

382 By incorporating the cellular growth dynamics under different seeding ratios, The
 383 PSMSR model has the potential to provide insights into the mechanism of phenotypic switching
 384 in response to a changing microenvironment (**Fig. 4D-I**). Here, we have calculated the
 385 emergence of tolerant cell population from sensitive cells or vice versa in both monotypic (**Fig.**
 386 **4D-E, Supplementary Fig. 11A, 11B, 11E and 11F**) and heterotypic cultures (**Fig. 4G-H,**
 387 **Supplementary Fig. 12A, 12B, 12F and 12G**). Of note, these cells are still experimentally
 388 detected as red or green, irrespective of their true phenotypes. Since in our model, stress is the
 389 driver for phenotypic switching, the switched phenotype cells only appear once stress builds up
 390 in the system over time (**Fig. 4I and Supplementary Fig. 12**). In both monotypic and heterotypic

391 cultures, the model predicts a rapid switch by the tolerant cells to the sensitive phenotype (up
392 to 97%, **Supplementary Fig. 11E, 12B, 12D** and **12G**), while maintaining a low but steady
393 tolerant population throughout the observations (**Fig. 4E, Supplementary Fig. 11B, 11F**). Thus,
394 we have seen how the cancer cells use phenotypic switching to maintain the overall fitness of
395 the community under different stress levels. To maintain steady growth, stress must be
396 mitigated, where switching to the tolerant phenotype pays off, since the tolerant cells are
397 capable of neutralizing stress. However, the fraction of tolerant phenotype in the population is
398 predicted to be low overall (10%, **Fig. 4G, Supplementary Fig. 12C** and **12H**). This may be due to
399 a balance between the necessity for stress removal and the energy or other costs required to
400 maintain the tolerant phenotype.

401 *Effects of phenotypic switching and stress give rise to diverse game-theoretical strategies in* 402 *mixed cell populations*

403 Cancer cell behavior is widely studied using game theory-based models where the inter-
404 species game strategies (competition and cooperation) are assumed to be constant throughout
405 the growth regime. A familiar example of such a model is the competitive Lotka-Volterra
406 equation, although more specialized models exist in the literature.²⁹ The phenotypic diversity
407 available to cancer cells suggest that their game strategic landscape will be considerably
408 complex, where the inter-species competition and cooperation are dynamically altered based
409 on changing scenarios.

410 Therefore, we have asked whether the PSMSR model can capture this complex strategic
411 landscape. Due to the complexity of the PSMSR equations, it is not possible to analytically
412 derive evolutionary payoffs (such as those given by the Lotka-Volterra equations³⁰). Moreover,
413 the payoffs are likely to vary over time, unlike in the classical game theoretical models, where
414 they are assumed to be constant. Therefore, we followed a different approach, where we
415 numerically fitted the Lotka-Volterra equation to the growth rates given by PSMSR over moving
416 time windows (**Supplementary Fig. 13**). At small (12 h) and very large time-windows (6 days),
417 the fitting seemed to be worse, while at moderate time windows such as 4-5 days, the fitting
418 appeared reasonable between the two models (**Supplementary Fig. 13**). By fitting the growth
419 rates obtained from the PSMSR model to the competitive Lotka-Volterra equations, we
420 determined the inter-species competition parameters as function of time, for different sensitive
421 to tolerant seeding ratios (**Fig. 4J and K**). **Fig. 4J** shows that the tolerant cells are initially
422 competitive towards the sensitive cells, but they become cooperative after 2-3 days of growth.
423 This coincides with the accumulation of stress (**Fig. 4G**) indicating that the microenvironment
424 plays a major role in altering the game strategies of the cancer phenotypes. Notably, the effect
425 of the sensitive cells towards the tolerant cells (**Fig. 4K**) is significantly smaller in magnitude.
426 Within the tumor, where the microenvironment is significantly more complex than our
427 experimental setup, multiple agents such as the various cancer-associated macrophages and
428 immune cells can dynamically alter the game strategies adopted by the tumor cells and steer
429 resistance evolution³¹. In summary, the PSMSR model, combined with the payoff calculation
430 scheme described above, demonstrates the diverse strategic landscape explored by the
431 sensitive and tolerant cells under varying cell population and stress levels.

432 *PSMSR model demonstrates the effectiveness of the intermittent cisplatin therapy*

433 Using the PSMSR model, we simulated the continuous and intermittent therapy
434 experiments, as explained before. We first calculated the model parameters by fitting to the
435 experimental growth trends measured in presence of cisplatin. The best agreement was
436 obtained when community cooperation such as phenotypic switching and stress removal were
437 turned off (**Fig. 5B and C**). This implies that high cisplatin levels trigger the tolerant cells to focus
438 on their own survival, similar to other social communities where imminent danger promotes
439 self-survival. Also, at high cisplatin levels, the phenotypic switching to sensitive is detrimental to
440 the survival of the community. Together, these observations are indicative of the adaptability of
441 the cancer cells for survival in adverse environments. In **Fig. 5D**, the magnitudes of the SCALE
442 parameter quantify the difference in cisplatin sensitivity between the sensitive and the tolerant
443 phenotypes.

444 Using the PSMSR model, we simulated the cisplatin dose cycles as explained in
445 **Supplementary Fig. 4**. Analogous to the experimental observations, the tolerant cell proportion
446 increased with time in the continuous therapy, while it remained relatively small and increased
447 at a slower rate during the intermittent cycles (**Fig. 5E-F**). Also, the intermittent 2 cycles of
448 cisplatin dosage created more tolerant cell population than the single cycle, in agreement with
449 the experiments (**Fig. 3D-F**). While the actual magnitudes of the tolerant cell population in the
450 simulations are different than in the experiments, the qualitative behaviors agree. The
451 quantitative difference between the predictions and the experiments could be partly attributed
452 to the growth attenuation due to confluence that is not accounted for by the PSMSR model.
453 Overall, these simulations show that the PSMSR model is able to qualitatively reproduce the
454 drug-induced behavior of the cancer cell population.

455 **Discussion**

456
457 Several studies have applied evolutionary game theory to cancer^{3-5,9,29,32-35} but as far as
458 we are aware, the adaptive strategies NSCLC cancer cells adopt in response to environmental
459 perturbations have not been investigated employing drug-naïve and drug-tolerant cells. We
460 demonstrated that the growth dynamics of these cells can only be explained by invoking
461 dynamic phenotypic switching upregulated by environmental stress. Consistent with this
462 assumption, the present data with the epigenetic regulator together with our previous
463 studies^{16,36} and those from others^{37,38}, strongly support the possibility that the two cell types
464 can stochastically switch their phenotypes via non-genetic mechanisms.

465 The present study also highlights the complex behavioral landscape of cancer cells,
466 where the payoff strategies are dynamically evolving via phenotypic plasticity induced by
467 environmental pressure (**Fig. 4J, K**). These inner level traits are cell frequency dependent and
468 can affect the carrying capacity of the population. The proposed PSMSR model can provide
469 important information about dynamic payoff strategies of multiple cellular phenotypes in a
470 time and frequency-dependent manner. In contrast, traditional evolutionary models (e.g., the
471 competitive LV) hold those payoffs to be fixed but are otherwise useful in understanding broad
472 game strategies of the system, due to their mathematical simplicity. Combining the PSMSR with

473 a model analogous to LV can thus give additional insight into the complex group behavior of
474 multiple cellular phenotypes including the role of the microenvironment, as was demonstrated
475 in **Fig. 4J** and **K**.

476 The mathematical modeling combined with the experimental observations
477 demonstrated that accumulated stress (induced by cell growth and microenvironment),
478 promotes phenotypic switching of sensitive cells to tolerant phenotypes. Thus, cells that switch
479 phenotypes help to partly neutralize the stress and allow the fast-growing sensitive cells to
480 proliferate, thereby sustaining the carrying capacity of the system. Thus, the resulting carrying
481 capacity is a function of both stress and the level of tolerant phenotype in the system.
482 Interestingly, the behavior of the tolerant cells appeared to be beneficial to the overall
483 community. They helped the proliferation of the sensitive cells by removing stress, and they
484 themselves adopt to a slower proliferation rate (when co-cultured for 3 weeks with the
485 sensitive cells, the parameter K_{G10} in **table 1**), so as to not compete for limited resources
486 (altruism). This altruistic behavior is even more beneficial in the crowded environment of a
487 tumor, where nutrients and oxygen could run low. The tolerant cells elucidated the
488 evolutionary strategy of bet-hedging where they display low evolutionary fitness under normal
489 conditions, but high fitness under stressful conditions, such as in presence of cisplatin.³⁹ The
490 intermittent therapy simulations show that the PSMSR model reproduces this behavior of the
491 tolerant cell population (**Fig. 5E-F**). Comparing the growth data with and without cisplatin in
492 conjunction with the PSMSR model, we also find that the phenotypic switching (and the
493 consequent altruism) may be turned off at high stress, when cisplatin is administered.
494 Therefore, it appears that the altruistic stress removal benefit by the tolerant cells could be
495 effective under normal conditions in the tumor, where a small tolerant cell population benefits
496 the drug-sensitive cells to sustain proliferation. However, under high stress of chemotherapy,
497 such stress removal mechanisms may be insufficient to sustain the sensitive cell viability. It is
498 therefore prudent to turn off phenotypic switching under such situations and allow the
499 sensitive cells to become extinct and the tolerant cells to proliferate. While bet-hedging
500 strategies by drug-tolerant phenotypes are well discussed in the literature³⁹, altruism by such
501 phenotypes has hitherto been unexplored. There is overwhelming evidence that such tolerant
502 persister phenotypes exist in the tumor in small proportions, even in non-drug-resistant
503 disease. However, it is not clear whether they have a specific ecological role other than adding
504 to the tumor heterogeneity, although recent evidence indicate that persisters can facilitate
505 escape from drug induced toxicity by reversibly switching to slow cycling phenotypes¹⁸.

506 Taken together, the behavior of the tolerant cells provides novel insights into the
507 phenotypic traits in cancer that emerge due to survival pressure as well as the cost-benefit
508 basis of such evolution. Of note, when co-cultured for 3 weeks prior to starting the experiment,
509 both the sensitive and tolerant cell types had equal opportunity to switch their strategy; either
510 they could have reduced or increased their proliferation rate to compete with each other, but
511 they followed an unexpected path where the sensitive cells remained unaffected and the
512 tolerant cells reduced their proliferation rate. This strategy could be helpful because most of
513 the genotoxic drugs used for chemotherapy target actively dividing cells. This behavior of
514 tolerant cells resembles phenotypic switching behavior reminiscent of persisters that are well
515 known in microbial systems⁴⁰ and more recently being recognized in cancer.^{39,41-43}

516 From a translational perspective, the present study also suggests that intermittent
517 rather than continuous chemotherapy may result in better outcomes in lung cancer. Although,
518 it may not cure the patient of the disease, it could potentially result in stable disease that can
519 be managed while sparing the patient of undesirable effects of excessive chemotherapy. The
520 fact that intermittent therapy has shown promise in other solid tumors^{7,9} should serve as a
521 motivation to try it in lung cancer.

522 **Materials and Methods**

523
524 The details of the cell lines, antibodies and reagents used, the protocol used for live cell
525 imaging, the ratios in which the heterotypic cultures were grown and observed in real time
526 along with the details of the zebrafish microinjection, drug treatment, and animal handling, are
527 provided in full detail in the Supplemental Section.

528 **Acknowledgments:** Work in the Salgia laboratory was supported by NIH grants R01CA218545
529 and R01CA247471. The illustration in Figs. 1 and 7G was created using the licensed software
530 from BioRender.

531 532 **References**

- 533
- 534 1. Alvarez-Arenas, A., Podolski-Renic, A., Belmonte-Beitia, J., Pesic, M., Calvo, G.F., (2019).
535 Interplay of Darwinian Selection, Lamarckian Induction and Microvesicle Transfer on Drug
536 Resistance in Cancer. *Sci Rep* 9, 9332.
 - 537 2. Salgia, R., Kulkarni, P., (2018). The Genetic/Non-genetic Duality of Drug 'Resistance' in
538 Cancer. *Trends Cancer* 4, 110-118.
 - 539 3. Wu, A., Liao, D., Tlsty, T.D., Sturm, J.C., Austin, R.H., (2014). Game theory in the death
540 galaxy: interaction of cancer and stromal cells in tumour microenvironment. *Interface focus* 4,
541 20140028.
 - 542 4. Kaznatcheev, A., Peacock, J., Basanta, D., Marusyk, A., Scott, J.G., (2019). Fibroblasts and
543 alectinib switch the evolutionary games played by non-small cell lung cancer. *Nature ecology &*
544 *evolution* 3, 450-456.
 - 545 5. Staňková, K., (2019). Resistance games. *Nature ecology & evolution* 3, 336-337.
 - 546 6. Mirnezami, R., Nicholson, J., Darzi, A., (2012). Preparing for precision medicine. *The New*
547 *England journal of medicine* 366, 489-91.
 - 548 7. Cunningham, J.J., Brown, J.S., Gatenby, R.A., Staňková, K., (2018). Optimal control to
549 develop therapeutic strategies for metastatic castrate resistant prostate cancer. *J Theor Biol*
550 459, 67-78.
 - 551 8. Stanková, K., Brown, J.S., Dalton, W.S., Gatenby, R.A., (2019). Optimizing Cancer
552 Treatment Using Game Theory: A Review. *JAMA oncology* 5, 96-103.
 - 553 9. Zhang, J., Cunningham, J.J., Brown, J.S., Gatenby, R.A., (2017). Integrating evolutionary
554 dynamics into treatment of metastatic castrate-resistant prostate cancer. *Nature*
555 *communications* 8, 1816.

- 556 10. Gatenby, R.A., Silva, A.S., Gillies, R.J., Frieden, B.R., (2009). Adaptive therapy. *Cancer*
557 *research* 69, 4894-4903.
- 558 11. Hata, A.N., Niederst, M.J., Archibald, H.L., Gomez-Caraballo, M., Siddiqui, F.M., Mulvey,
559 H.E., Maruvka, Y.E., Ji, F., Bhang, H.-e.C., Krishnamurthy Radhakrishna, V., et al., (2016). Tumor
560 cells can follow distinct evolutionary paths to become resistant to epidermal growth factor
561 receptor inhibition. *Nature medicine* 22, 262-269.
- 562 12. Venkatesan, S., Swanton, C., Taylor, B.S., Costello, J.F., (2017). Treatment-Induced
563 Mutagenesis and Selective Pressures Sculpt Cancer Evolution. *Cold Spring Harb Perspect Med* 7,
564 a026617.
- 565 13. Bottery, M.J., Pitchford, J.W., Friman, V.-P., (2020). Ecology and evolution of
566 antimicrobial resistance in bacterial communities. *The ISME Journal*.
- 567 14. Grolmusz, V.K., Chen, J., Emond, R., Cosgrove, P.A., Pflieger, L., Nath, A., Moos, P.J., Bild,
568 A.H., (2020). Exploiting collateral sensitivity controls growth of mixed culture of sensitive and
569 resistant cells and decreases selection for resistant cells in a cell line model. *Cancer Cell*
570 *International* 20, 253.
- 571 15. Marusyk, A., Tabassum, D.P., Altrock, P.M., Almendro, V., Michor, F., Polyak, K., (2014).
572 Non-cell-autonomous driving of tumour growth supports sub-clonal heterogeneity. *Nature* 514,
573 54-8.
- 574 16. Mohanty, A., Nam, A., Pozhitkov, A., Yang, L., Srivastava, S., Nathan, A., Wu, X.,
575 Mambetsariev, I., Nelson, M., Subbalakshmi, A.R., et al., (2020). A Non-genetic Mechanism
576 Involving the Integrin beta4/Paxillin Axis Contributes to Chemoresistance in Lung Cancer.
577 *iScience* 23, 101496.
- 578 17. Boumahdi, S., de Sauvage, F.J., (2020). The great escape: tumour cell plasticity in
579 resistance to targeted therapy. *Nat Rev Drug Discov* 19, 39-56.
- 580 18. Mullard, A., (2020). Stemming the tide of drug resistance in cancer. *Nat Rev Drug Discov*
581 19, 221-223.
- 582 19. Babbs, C.F., (2012). Predicting success or failure of immunotherapy for cancer: insights
583 from a clinically applicable mathematical model. *Am J Cancer Res* 2, 204-213.
- 584 20. Momeni, B., Xie, L., Shou, W., (2017). Lotka-Volterra pairwise modeling fails to capture
585 diverse pairwise microbial interactions. *Elife* 6, e25051.
- 586 21. Vet, S., de Buyl, S., Faust, K., Danckaert, J., Gonze, D., Gelens, L., (2018). Bistability in a
587 system of two species interacting through mutualism as well as competition: Chemostat vs.
588 Lotka-Volterra equations. *PLOS ONE* 13, e0197462.
- 589 22. Li, X.Y., Pietschke, C., Fraune, S., Altrock, P.M., Bosch, T.C.G., Traulsen, A., (2015). Which
590 games are growing bacterial populations playing? *J R Soc Interface* 12.
- 591 23. Carvalho, G., Guilhen, C., Balestrino, D., Forestier, C., Mathias, J.-D., (2017). Relating
592 switching rates between normal and persister cells to substrate and antibiotic concentrations: a
593 mathematical modelling approach supported by experiments. *Microbial Biotechnology* 10,
594 1616-1627.
- 595 24. Ozawa, S., Sugiyama, Y., Mitsuhashi, Y., Kobayashi, T., Inaba, M., (1988). Cell killing
596 action of cell cycle phase-non-specific antitumor agents is dependent on concentration--time
597 product. *Cancer Chemother Pharmacol* 21, 185-90.
- 598 25. Nagai, N., Ogata, H., (1997). Quantitative relationship between pharmacokinetics of
599 unchanged cisplatin and nephrotoxicity in rats: importance of area under the concentration-

600 time curve (AUC) as the major toxicodynamic determinant in vivo. *Cancer Chemother*
601 *Pharmacol* 40, 11-8.

602 26. El-Kareh, A.W., Secomb, T.W., (2003). A mathematical model for cisplatin cellular
603 pharmacodynamics. *Neoplasia* 5, 161-9.

604 27. Goldberg, D.E., *Genetic Algorithms in Search, Optimization and Machine Learning*.
605 Addison-Wesley Longman Publishing Co., Inc.: 1989.

606 28. Scrucca, L., (2013). GA: A Package for Genetic Algorithms in R. 2013 53, 37.

607 29. Kareva, I., Karev, G., (2019). Natural Selection Between Two Games with Applications to
608 Game Theoretical Models of Cancer. *Bulletin of mathematical biology* 81, 2117-2132.

609 30. Bomze, I.M., (1983). Lotka-Volterra equation and replicator dynamics: A two-
610 dimensional classification. *Biological Cybernetics* 48, 201-211.

611 31. Bhattacharya, S., Mohanty, A., Achuthan, S., Kotnala, S., Jolly, M.K., Kulkarni, P., Salgia,
612 R., (2021). Group Behavior and Emergence of Cancer Drug Resistance. *Trends Cancer* 7, 323-
613 334.

614 32. You, L., Brown, J.S., Thuijsman, F., Cunningham, J.J., Gatenby, R.A., Zhang, J., Staňková,
615 K., (2017). Spatial vs. non-spatial eco-evolutionary dynamics in a tumor growth model. *J Theor*
616 *Biol* 435, 78-97.

617 33. Swierniak, A., Krzeslak, M., Borys, D., Kimmel, M., (2018). The role of interventions in
618 the cancer evolution-an evolutionary games approach. *Mathematical biosciences and*
619 *engineering* : MBE 16, 265-291.

620 34. West, J., Robertson-Tessi, M., Luddy, K., Park, D.S., Williamson, D.F.K., Harmon, C.,
621 Khong, H.T., Brown, J., Anderson, A.R.A., (2019). The Immune Checkpoint Kick Start:
622 Optimization of Neoadjuvant Combination Therapy Using Game Theory. *JCO clinical cancer*
623 *informatics* 3, 1-12.

624 35. Wu, A., Liao, D., Austin, R., (2015). Evolutionary game theory in cancer: first steps in
625 prediction of metastatic cancer progression? *Future Oncol* 11, 881-3.

626 36. Mooney, S.M., Jolly, M.K., Levine, H., Kulkarni, P., (2016). Phenotypic plasticity in
627 prostate cancer: role of intrinsically disordered proteins. *Asian journal of andrology* 18, 704-10.

628 37. Goldman, A., Majumder, B., Dhawan, A., Ravi, S., Goldman, D., Kohandel, M., Majumder,
629 P.K., Sengupta, S., (2015). Temporally sequenced anticancer drugs overcome adaptive
630 resistance by targeting a vulnerable chemotherapy-induced phenotypic transition. *Nature*
631 *communications* 6, 6139.

632 38. Gupta, P.B., Fillmore, C.M., Jiang, G., Shapira, S.D., Tao, K., Kuperwasser, C., Lander, E.S.,
633 (2011). Stochastic state transitions give rise to phenotypic equilibrium in populations of cancer
634 cells. *Cell* 146, 633-44.

635 39. Jolly, M.K., Kulkarni, P., Weninger, K., Orban, J., Levine, H., (2018). Phenotypic Plasticity,
636 Bet-Hedging, and Androgen Independence in Prostate Cancer: Role of Non-Genetic
637 Heterogeneity. *Front Oncol* 8, 50.

638 40. Brauner, A., Fridman, O., Gefen, O., Balaban, N.Q., (2016). Distinguishing between
639 resistance, tolerance and persistence to antibiotic treatment. *Nature reviews. Microbiology* 14,
640 320-30.

641 41. Dawson, C.C., Intapa, C., Jabra-Rizk, M.A., (2011). "Persisters": survival at the cellular
642 level. *PLoS pathogens* 7, e1002121.

643 42. Hata, A.N., Niederst, M.J., Archibald, H.L., Gomez-Caraballo, M., Siddiqui, F.M., Mulvey,
644 H.E., Maruvka, Y.E., Ji, F., Bhang, H.E., Krishnamurthy Radhakrishna, V., et al., (2016). Tumor
645 cells can follow distinct evolutionary paths to become resistant to epidermal growth factor
646 receptor inhibition. *Nature medicine* 22, 262-9.
647 43. Vallette, F.M., Olivier, C., Lézot, F., Oliver, L., Cochonneau, D., Lalier, L., Cartron, P.F.,
648 Heymann, D., (2019). Dormant, quiescent, tolerant and persister cells: Four synonyms for the
649 same target in cancer. *Biochemical pharmacology* 162, 169-176.
650 55. Li, X.-Y., Pietschke, C., Fraune, S., Altrock, P. M., Bosch, T. C. G., & Traulsen, A. (2015).
651 Which games are growing bacterial populations playing? *Journal of the Royal Society Interface*,
652 12(108), 20150121-10.
653

654 **Figure Legends**

655

656 **Figure 1. Schematic summarizing the experiment and the source of data used in developing**
657 **the theoretical cell growth models. (A)** The schematic representation of the different
658 incubation duration, ratios, and treatments used for generating the data to develop the
659 mathematical model. **(B)** schematic describing the principles based on which the mathematical
660 model PSMSR was developed; **(C)** panel representing the functional form of PSMSR (please see
661 the main text for further details).
662

663 **Figure 2. Behavior of cisplatin-sensitive (S) and tolerant (T) NSCLC cells in 2D co-culture. (A)**
664 Schematic representation of the experimental design of co-culturing S and T cells in a ratio of
665 1:1 and collection of data points. Proliferation of sensitive (red) and tolerant (green) cells under
666 different culture conditions in the absence or presence of cisplatin. Two-way ANOVA test
667 (multiple comparison) showing statistical significance **** $p < 0.0001$. **(B)** Sensitive and tolerant
668 cells were plated in increasing T:S ratios and cultured for 3 weeks. Proliferation rate of sensitive
669 cells (red) and tolerant cells (green) in heterotypic culture over the course of 144 hours. **(C)** Fold
670 change in cell count of sensitive cells (red) and tolerant cells (green) in heterotypic culture was
671 measured after 144 hours for ratios 1:1, 2:1, 4:1 and 8:1. Two-way ANOVA was used for
672 calculating statistical significance **** $p < 0.0001$, ns-not significant. **(D)** Fold change in cell count
673 of sensitive cells (purple) and tolerant cells (blue) in heterotypic culture was measured after
674 144 hours in presence of cisplatin for ratios 1:1, 2:1, 4:1 and 8:1. Two-way ANOVA was used for
675 calculating statistical significance **** $p < 0.0001$, ns-not significant. **(E)** Change in
676 tolerant/sensitive cells ratio with (orange) and without (black) 5 μ M cisplatin over the course of
677 144 hours was measured. **(F)** Schematic representation of the conditioned medium experiment.
678 **(G)** The left line graph representing the effect of tolerant cell conditioned medium on sensitive
679 cells, and the right line graph representing the inhibitory effect of tolerant cell conditioned
680 medium on sensitive cells growth. **(H)** Schematic representation of conditioned medium
681 experiment to correlate the stoichiometry between cell number and inhibitory effect secreted
682 by sensitive cells. **(I)** The bar graph representing the inhibitory effect of condition medium on
683 different cell number of tolerant or sensitive cells. Statistical significance information can be
684 found in **Supplementary Table 2 and 3**.
685

686 **Figure 3. Tolerant cells reversibly switch their phenotype to become sensitive with**
687 **intermittent therapy. (A-C)** Bar graph showing the ratio of tolerant versus sensitive cell
688 population over a period of 10 days. The cell ratio for the “Continuous” group wherein the cells
689 were continuously treated with cisplatin is shown in blue and the ratio for the “Intermittent”
690 group wherein the cells were treated with cisplatin for 2 days and released in fresh medium
691 (intermittent) is shown in black. **(D-F)** Media from “Intermittent – 2 cycles” group was removed
692 after 4 days of cisplatin treatment and replaced with fresh medium and the cells were allowed
693 to grow until confluent. These cells were monitored in real-time to determine the ratio of
694 tolerant vs sensitive over the course of 25 days. Similarly, the cells that only received cisplatin
695 once (“Intermittent – 1 cycle”) throughout the experiment were also followed for 25 days. **(G)**
696 Sensitive (S, red fluorescence) and tolerant (T, green fluorescence) cells were mixed at S:T ratio
697 of 4:1 and microinjected into the perivitelline space of zebrafish larvae 48 h post fertilization
698 (hpf). Twenty-four hours after microinjection, larvae were randomly divided into 3 groups:
699 Group 1 received no drug treatment (Untreated), Group 2 received cisplatin 20 μ M for 3 days
700 and released with no drug for 2 days (Intermittent), and Group 3 received cisplatin 20 μ M
701 continuously for 5 days (Continuous). Ratio of tolerant versus sensitive cells was determined by
702 measuring fluorescence intensity. **(H)** Effect of suberoylanilide hydroxamic acid (SAHA) on
703 cisplatin-sensitive (H23), tolerant (H2009), and resistant (H1993) cells, demonstrating that
704 tolerant cells can reversibly switch their phenotype to become sensitive. Statistical significance
705 information can be found in **Supplementary Table 4**.

706
707 **Figure 4. Cooperativity and stress response as described by the PSMSR model. (A)** Schematic
708 describing the PSMSR model; initially, the sensitive and the tolerant cells proliferate
709 independently; as stress builds up, sensitive cells switch their phenotype to tolerant cells and
710 vice versa; tolerant cells remove stress and maintain a small population, while enabling the
711 sensitive cells to proliferate. **(B-C)** Fitting of the phenotype-switch model to the cellular growth
712 curves of sensitive and tolerant cell populations, where the cells were mixed at different
713 proportions and counting was started immediately; the colors represent the growth curves
714 from different initial seeding proportions, as indicated in the legend (sensitive to tolerant cell
715 seeding ratios); **(D-F)** predicted evolution of phenotypic switching and stress in monotypic
716 cultures; (D-E) populations of sensitive and (switched) tolerant phenotypes with time, when
717 seeded with sensitive cells only; (F) stress as function of time; **(G-I)** predicted evolution of
718 switched phenotypes and stress in heterotypic culture experiments, where cell growth was
719 monitored immediately after mixing; (G) fraction of sensitive cells that have switched to the
720 tolerant phenotype, as function of time; (H) fraction of tolerant cells that have switched to the
721 sensitive phenotype, as function of time; (I) stress with time; colors are according to the initial
722 seeding ratio of sensitive to tolerant cells as shown in the legend; the total cell population in
723 each case was close to 5000; **(J-K)** evolving game strategy landscape of cellular population due
724 to stress and phenotypic switching; the heatmaps of time varying payoff values representative
725 of inter-species competition/cooperation are shown as function of sensitive to tolerant seeding
726 ratio; payoff values are derived by fitting the PSMSR model to the competitive Lotka-Volterra
727 equations; orange areas in the maps represent competitive behavior, green areas represent
728 cooperative behavior; (J) α_{12} representing the effect of tolerant cells towards the sensitive cells;
729 (K) α_{21} representing the effect of sensitive cells towards the tolerant cells.

730
 731
 732
 733
 734
 735
 736
 737
 738
 739
 740
 741
 742
 743
 744
 745

Figure 5. Mathematical model for cisplatin resistance. (A) Schematic demonstration of AUC and cellular death rate as function of AUC; (B-C) fitting of the experimental growth data where the cells were co-cultured for three weeks; B: sensitive cells; C: tolerant cells; circles and lines represent the experimental and fitted trends respectively; (D) SCALE parameter as measure of cisplatin sensitivity for the sensitive and the tolerant cells; the error bars represent 95% confidence limits (E-F) simulation of intermittent and continuous cisplatin treatment according to the protocols described in Fig. 3; the initial sensitive to tolerant cell ratio was set to 4:1 with a total cell population of 50,000. (G) An illustrative model depicting the presence (and absence) of group behavior among sensitive and tolerant cells under varying conditions of stress and effects of continuous versus intermittent therapy.

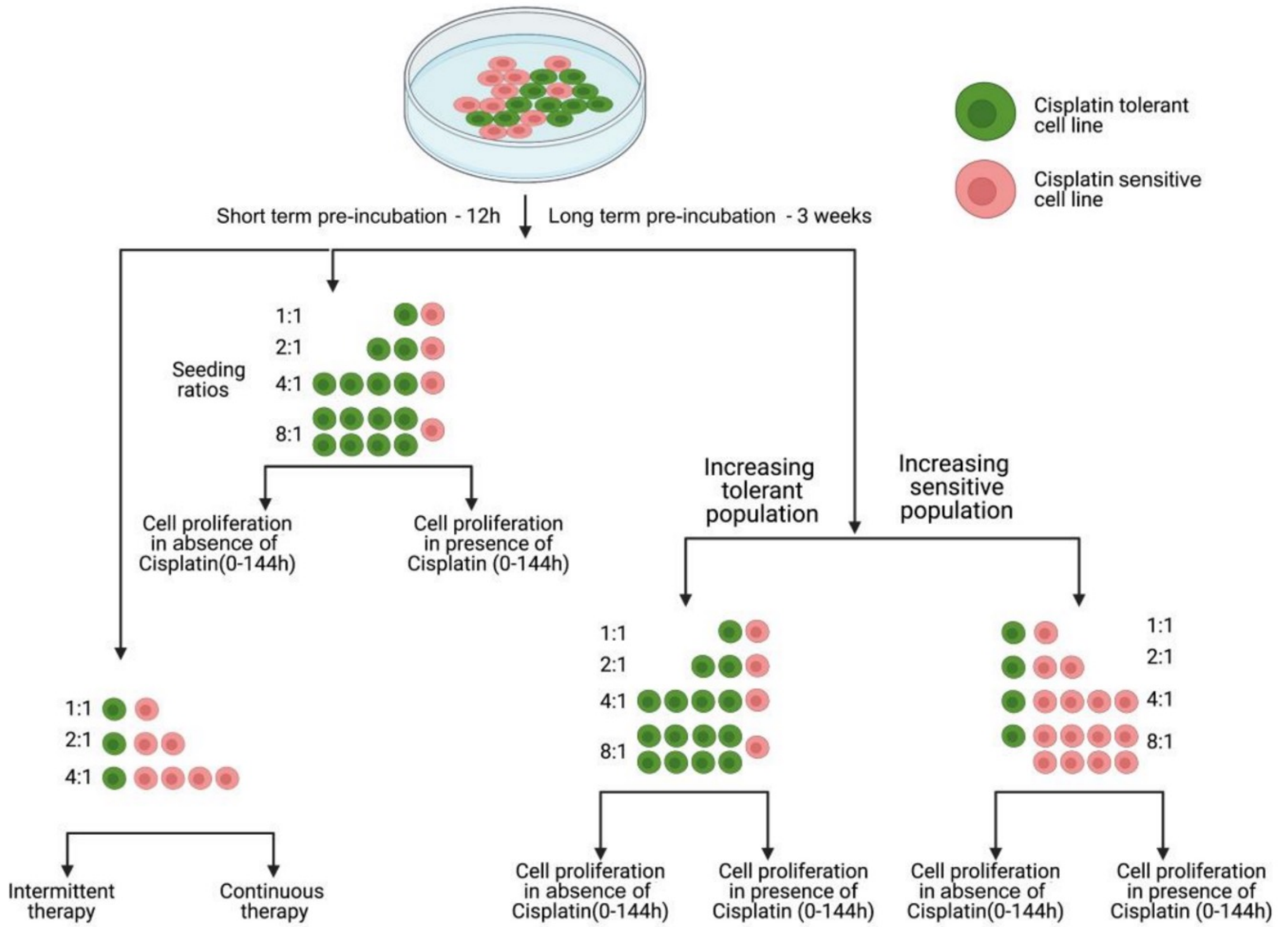
Table 1: Model parameters and parameter search ranges for PSMSR, including the 95% confidence limits.

| Condition | K_0 | K_b | K_{G0} | K_{G10} | K_{str} | $K_{str,d}$ | a | b | g | S_{drug} | AUC_s^5 | AUC_s^{95} | $SCALE_s$ | AUC_t^5 | AUC_t^{95} | $SCALE_t$ |
|-------------------------------------|------------------|-----------|-------------|-------------|--|---|------------------|------------------|------------------|------------|-----------|--------------|-----------|-----------|--------------|-----------|
| Heterotypic | 0.049 ±0.0003 | 3.57±0.02 | 0.713±0.001 | 0.687±0.004 | 7.14×10^{-4} ± 3×10^{-6} | 5.64×10^{-3} ± 4×10^{-5} | 0.046 ±0.0004 | 0.038 ±0.0002 | 0.018 ±0.0006 | | | | | | | |
| Heterotypic, 3 weeks | 0.052 ±0.0007 | 2.6±0.05 | 0.708±0.002 | 0.189±0.016 | 6.74×10^{-4} ± 8×10^{-6} | 5.52×10^{-3} ± 1×10^{-4} | 0.05 ±0.001 | 0.038 ±0.0006 | 0.02 ±0.0006 | | | | | | | |
| Heterotypic, cisplatin 5µM | 0.033 ±0.0017 | 0 | 1.033±0.046 | 0.976±0.054 | 5.9×10^{-4} ± 2.8×10^{-5} | 0 | NA | 0.04 ±0.003 | 0.034 ±0.003 | 108±14.5 | 239±12 | 1153±58 | 8.61±0.5 | 233±17 | 1201±49 | 5.79±0.6 |
| Heterotypic, 3 weeks, cisplatin 5µM | 0.033 ±0.0015 | 0 | 0.966±0.05 | 0.967±0.05 | 5.8×10^{-4} ± 3.3×10^{-5} | 0 | NA | 0.039 ±0.002 | 0.036 ±0.003 | 96.8±9.95 | 271±14 | 1098±44 | 8.91±0.5 | 250±14 | 1098±47 | 6.89±0.7 |
| Parameter search range | 0-0.1 | 0-5 | 0-2 | 0-2 | 0-0.001 | 0-0.02 | 0-0.1 | 0-0.1 | 0-0.1 | 1-500 | 1-500 | 10-1500 | 0.1-20 | 1-500 | 10-1500 | 0.1-20 |

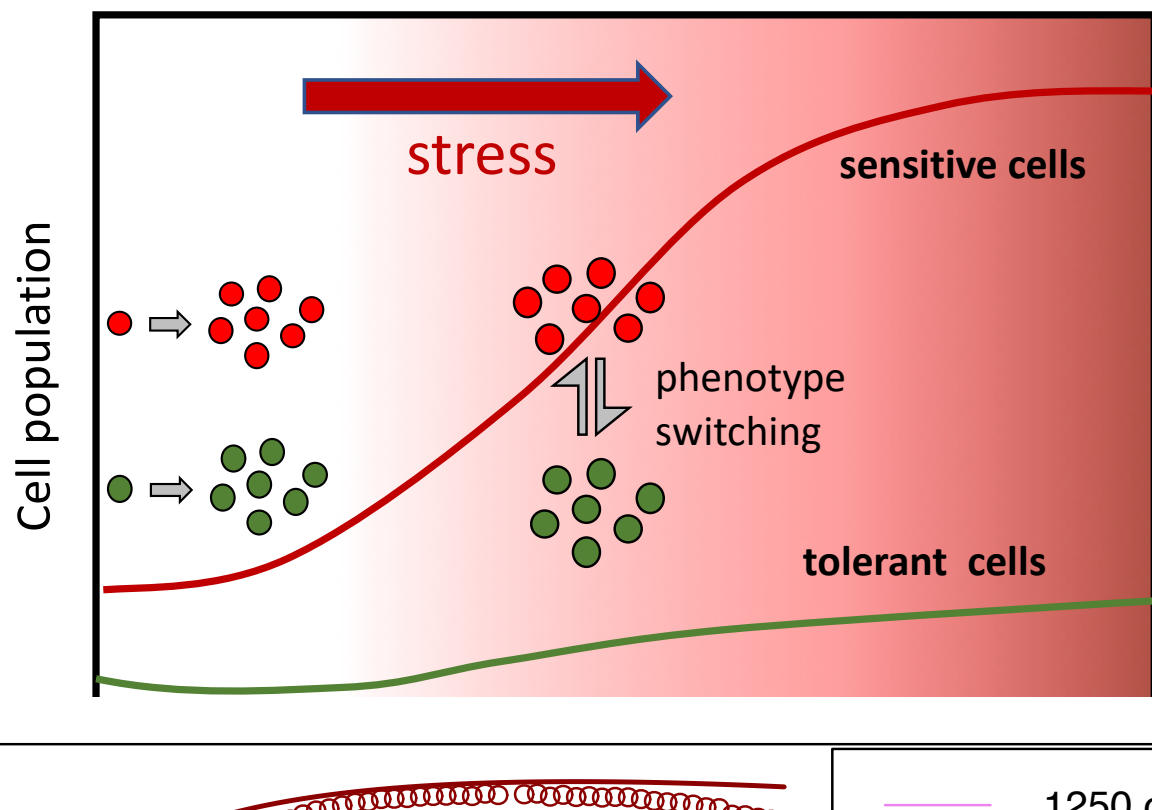
746

Figure 1

A



B



C

Phenotype Switch Model with Stress Response (PSMSR)

$$\frac{dS}{dt} = -K_a S + K_b T + K_{GS} S$$

sensitive

$$\frac{dT}{dt} = -K_b T + K_a S + K_{GT} T$$

tolerant

net growth phenotype switching proliferation

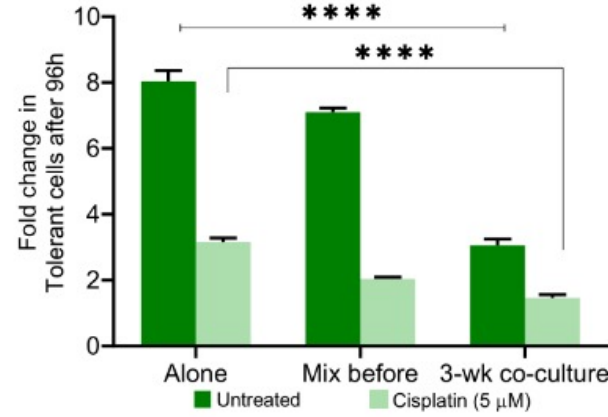
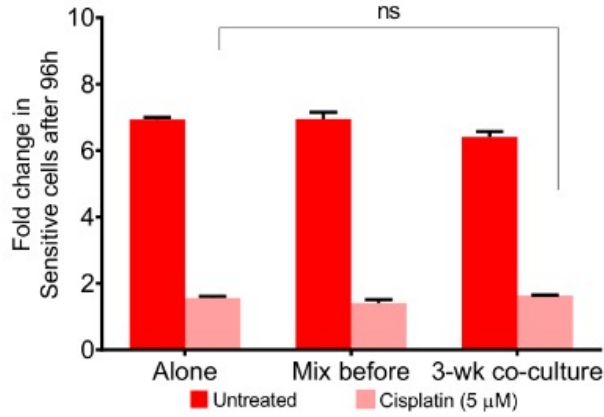
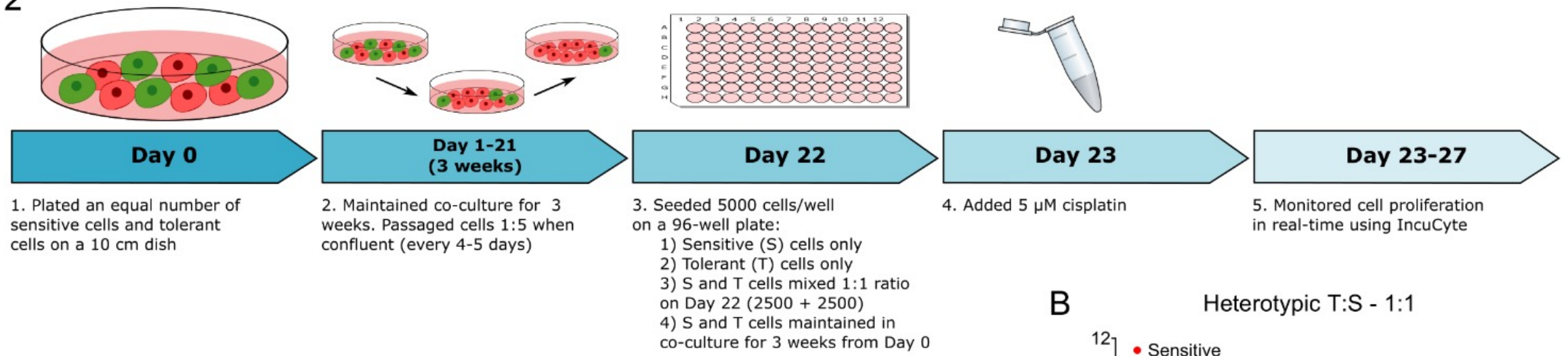
$$\frac{dC_{Str}}{dt} = K_{Str} S - K_{Str,d} T$$

stress

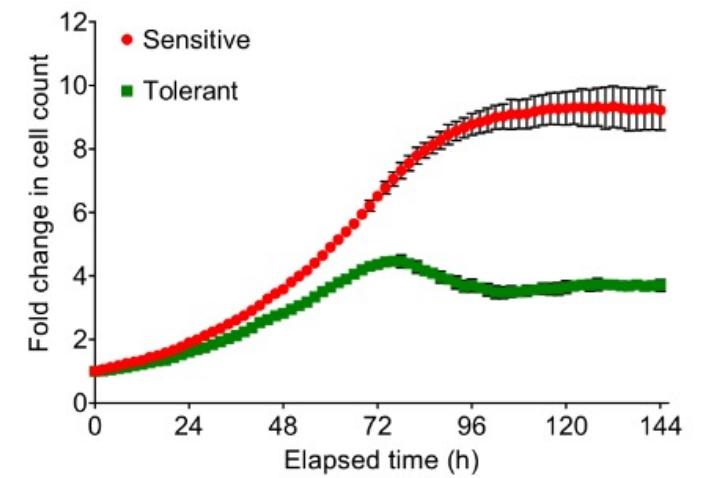
generation removal

Fig. 2

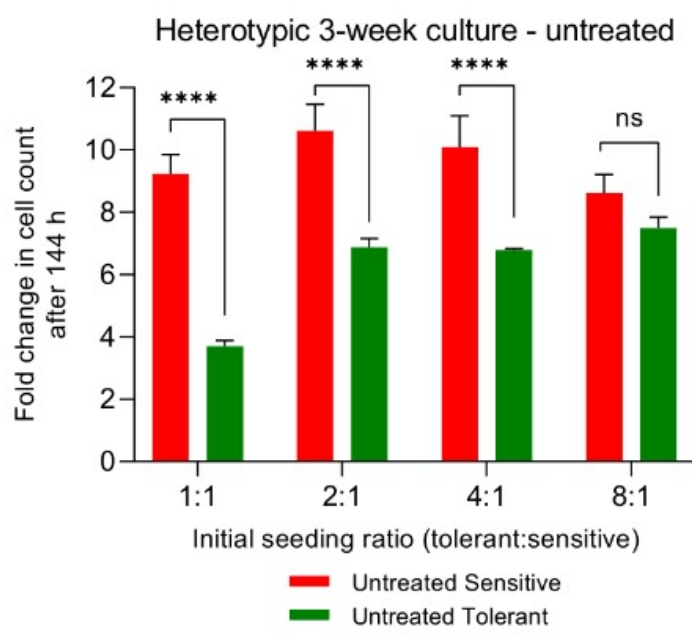
A



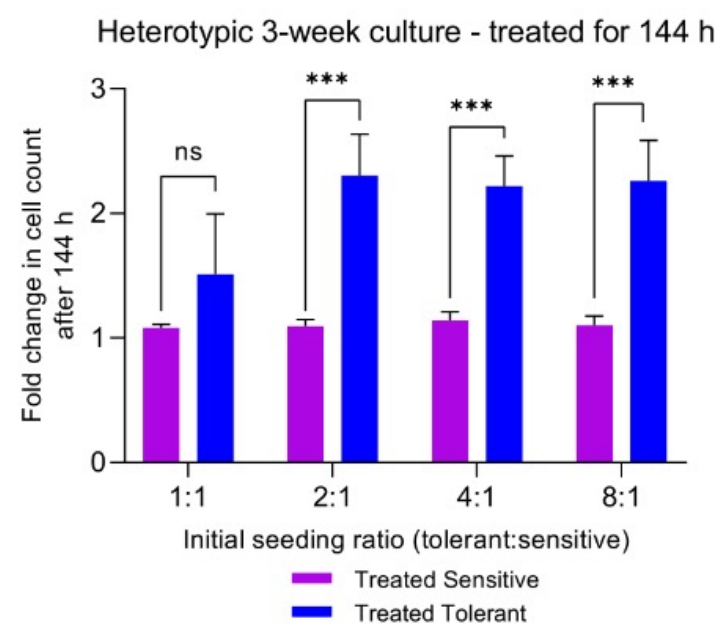
B Heterotypic T:S - 1:1



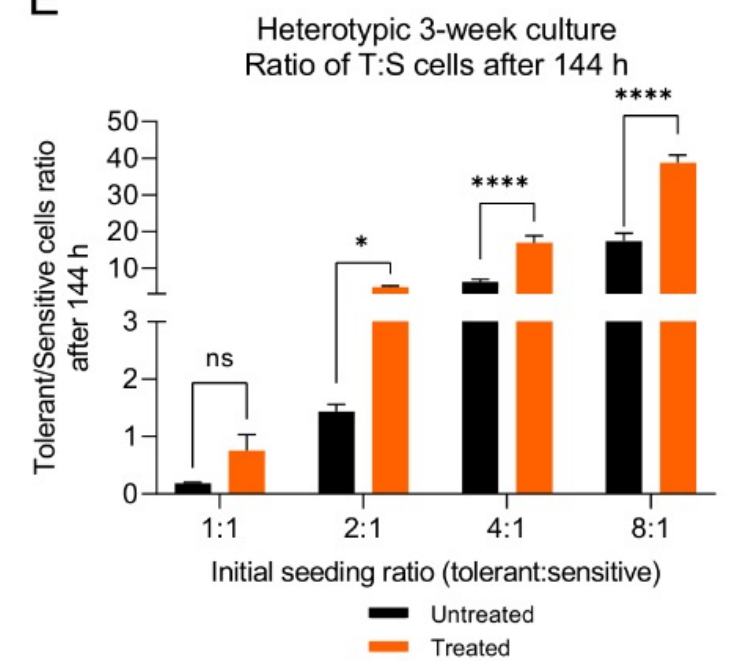
C



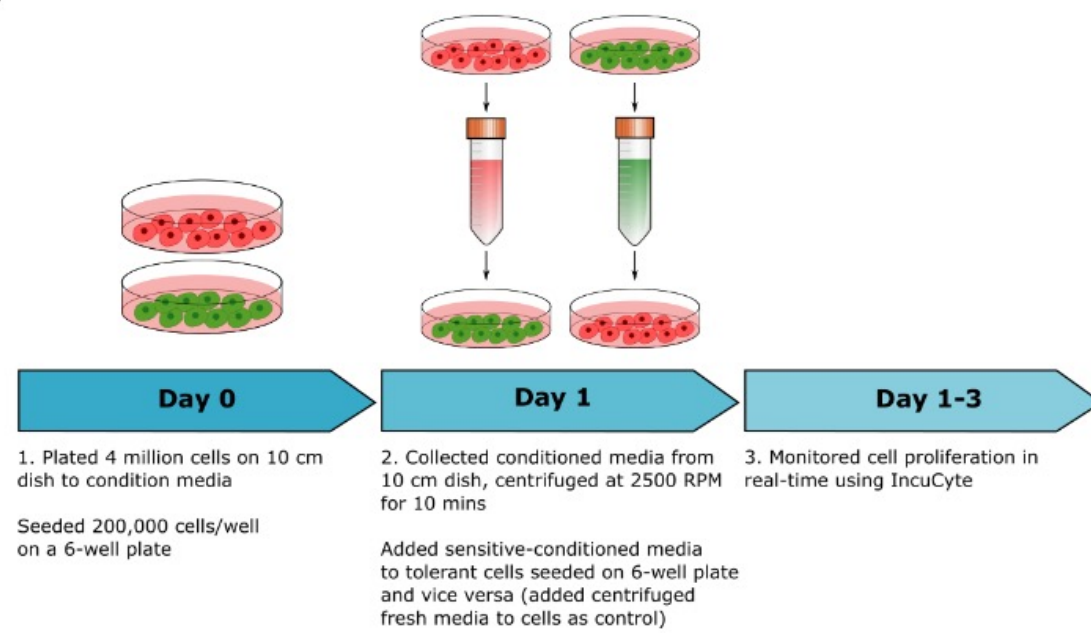
D



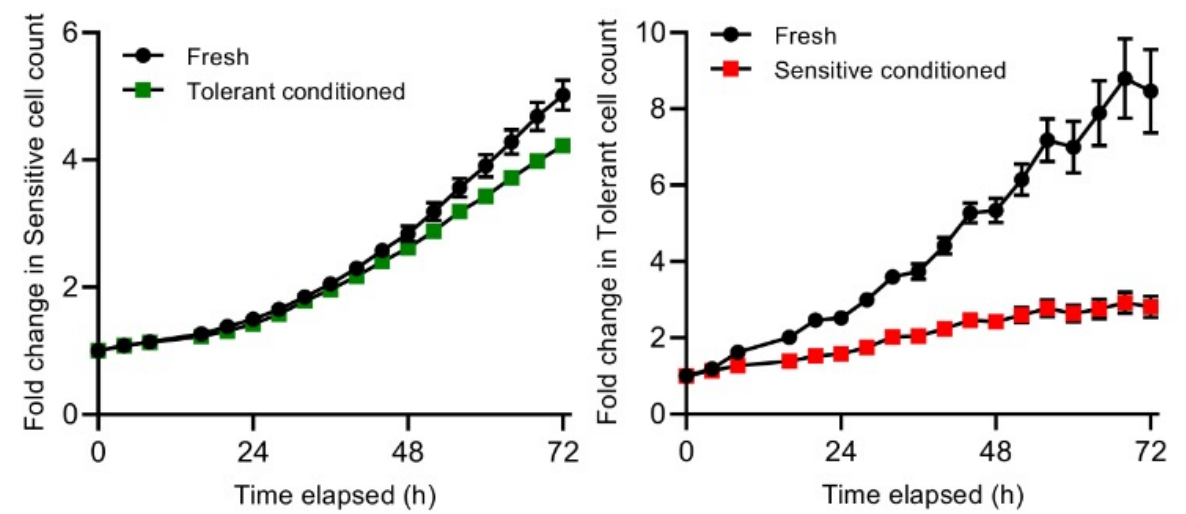
E



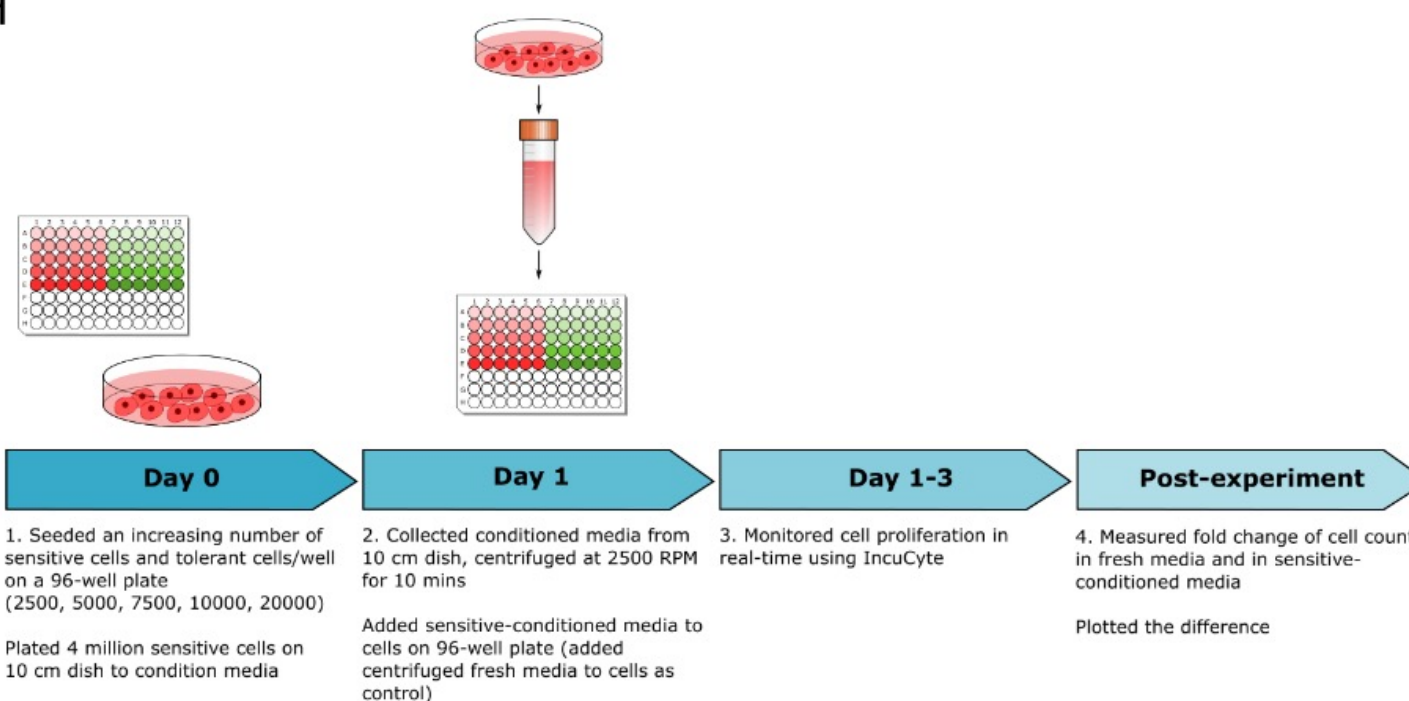
F



G



H



I

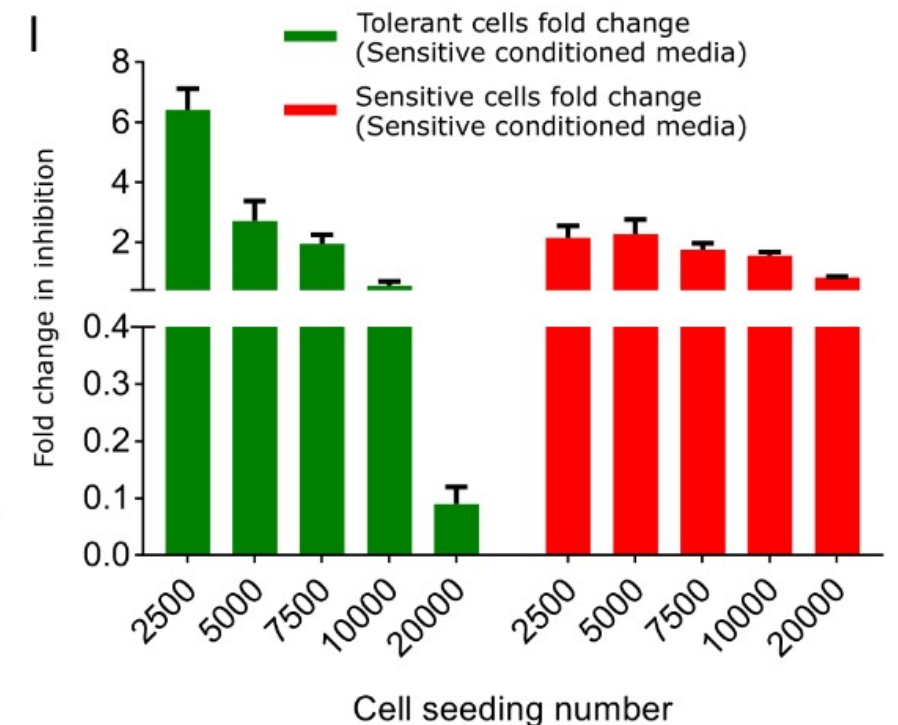


Fig. 3

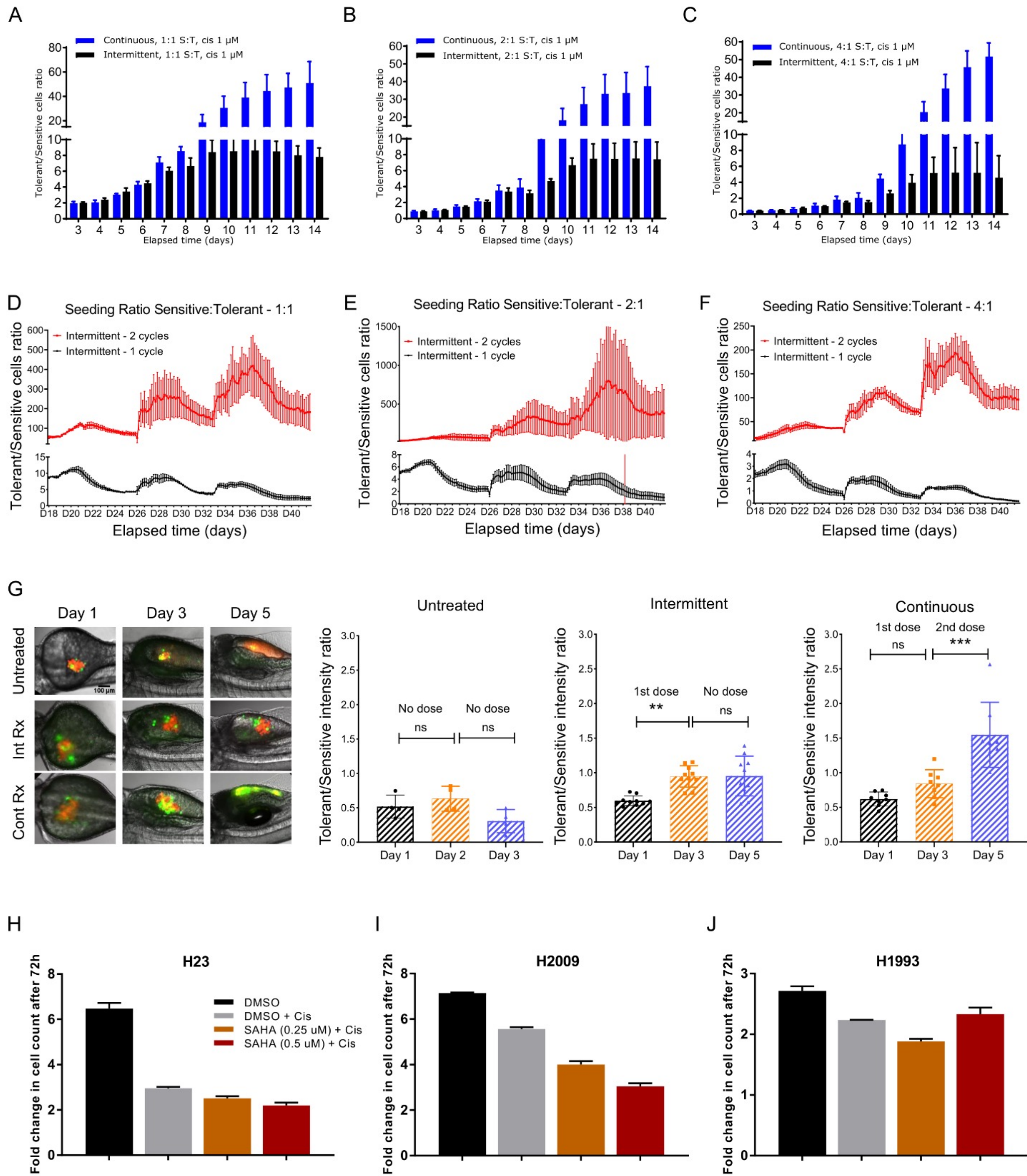


Figure 4

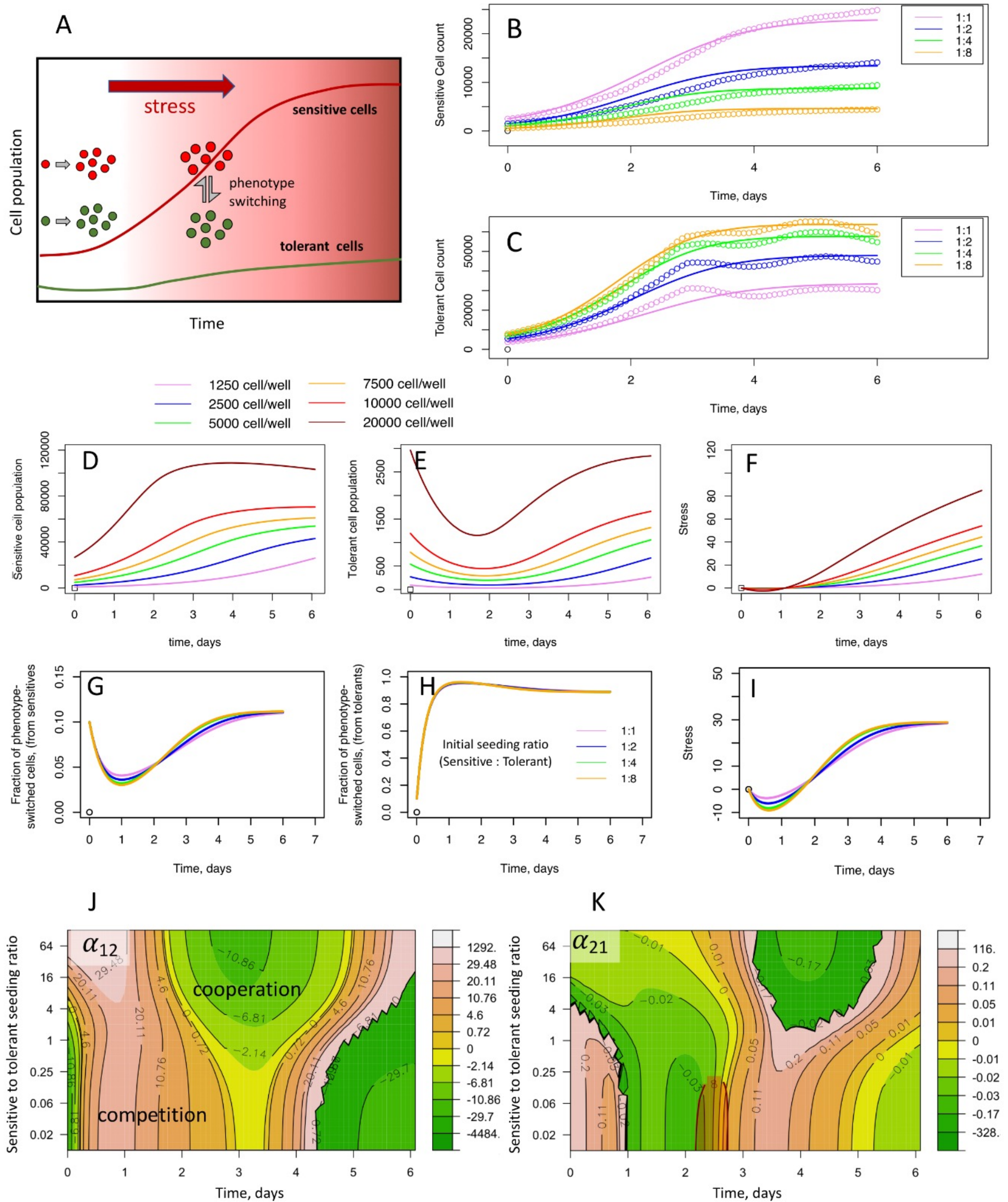


Figure 5

